*Tellus (2004), 56A, 308–327*
*Printed in UK. All rights reserved*


**TELLUS**

# Evaluating climate model simulations of tropical cloud

*By* MARK A. RINGER* and RICHARD P. ALLAN†, *Met Office, Hadley Centre for Climate Prediction and Research, FitzRoy Road, Exeter, EX1 3PB, United Kingdom*

(Manuscript received 10 June 2003; in final form 28 December 2003)

ABSTRACT

The representation of tropical cloud and its radiative effects in the Hadley Centre climate model are evaluated using a combination of Earth observation data and meteorological reanalyses. It is shown that useful information regarding the model's physical parametrizations can be obtained by considering cloud radiative effects and cloud types in terms of 'dynamical regimes', defined in terms of sea surface temperature and large-scale vertical motion. In addition to comparisons with observed top-of-atmosphere radiation budget parameters and total cloud amount, information is obtained through direct comparisons of International Satellite Cloud Climatology Project (ISCCP) cloud types, defined according to cloud top pressure and optical depth, with corresponding model diagnostics. An analysis of the atmosphere-only model, HadAM3, demonstrates how errors in the albedo and outgoing long-wave radiation can be related to the simulation of particular cloud types in the different dynamical regimes. Inconsistencies between the simulations of the various cloud types and the top-of-atmosphere radiation budget are also highlighted. A version of the model including several new cloud-related parametrizations is then examined. A more consistent comparison with the observed radiation budget and cloud amounts is obtained, although deficiencies in the simulation still remain. A parametrization for the radiative effects of convective anvils and the impact of a new boundary layer mixing scheme are examined in more detail. Finally, it is shown how the climate model's ability to simulate the observed interannual variability of cloud in the equatorial Pacific follows directly from the analysis according to dynamical regimes.

## 1. Introduction

The distribution and properties of cloud in the tropics depend on complex relationships between the thermodynamic structure of the atmosphere and the large-scale circulation. Moreover, the interaction between the cloud systems themselves and the circulation influences the temperature and moisture structure of the tropical atmosphere and, consequently, the climate of the Earth as a whole. It is therefore important that climate models be able to represent both the physical processes which determine the cloud distribution, such as convection and boundary-layer processes, and the influence of clouds, for example cloud radiative effects, on the climate system.

Satellite observations such as the Earth Radiation Budget Experiment (ERBE) and the International Satellite Cloud Climatology Project (ISCCP) have demonstrated the wide variety of cloud types and their associated radiative properties to be found in the tropics. These cloud types are known to be related to the prevailing dynamical conditions. For example, optically thick deep convective cloud, which has strong effects in both the short-wave (SW) and long-wave (LW) parts of the spectrum, occurs over the warmest waters in areas of strong ascending motion (e.g. the western Pacific 'warm pool'), whereas low-level boundary layer cloud, which has a strong SW cooling effect but only a weak LW effect, typically forms in areas of subsidence over cooler sea surface temperature (SSTs), e.g. the equatorial Pacific 'cold tongue'.

This link between the cloud distribution and the large-scale circulation suggests a methodology for considering tropical clouds in terms of dynamics and subsequently applying the same techniques to assess model simulations. Previous observational studies (e.g. Fu et al., 1994; Bony et al., 1997b; Lau et al., 1997) have demonstrated that separating the influence of local SST and the large-scale circulation provides a useful framework for studying tropical cloud and its radiative effects. Similar techniques have been used to assess the observed relationships between tropical cloud and SST (Bony et al., 1997b), the representation of El Niño Southern Oscillation (ENSO) related cloud variations in climate models (Allan et al., 2002) and the influence of dynamics on the cloud response to climate change (Bony et al., 2003; Williams et al., 2003). In a related study Webb et al., (2001) compared the representation of cloud and cloud radiative effects in three climate models and demonstrated the value of simulating cloud amounts in cloud top pressure (CTP) and optical thickness categories defined by ISCCP. This allowed direct comparisons between the ISCCP data and the models and also served to highlight the necessity of correctly representing the

*Corresponding author.
e-mail: mark.ringer@metoffice.com
†Present affiliation: ESSC, University of Reading, UK.

influence of the different cloud types on the top-of-atmosphere radiation budget. Subsequently, the studies of Norris and Weaver (2001) and Tselioudis and Jakob (2002) combined this approach with an evaluation in terms of dynamical regimes in order to assess model simulations of mid-latitude cloud. These techniques contrast with the more usual method of simply comparing observed and model climatologies of cloud amounts and radiative fluxes and represent a more process-oriented approach to assessing a model's physical parametrizations which helps to identify sources of error more clearly.

In this paper we present an assessment of the simulation of tropical cloud in the Hadley Centre climate model. The representation of cloud properties and cloud radiative effects is evaluated according to 'dynamical regimes', defined in terms of the SST and the large-scale circulation. Present-day climate model simulations are compared with observations using a combination of satellite data sets of radiation budget and clouds together with meteorological reanalyses. The analysis in terms of dynamical regimes is augmented by including direct comparisons of ISCCP cloud types with simulations in different versions of the model. The principal aims of this study are: to provide a thorough evaluation of tropical cloud in the Hadley Centre climate model; to show how the dynamical regimes framework allows the impacts of new physical parametrizations to be assessed more easily; and to demonstrate how the information gained from this analysis relates to the model's simulation of climate variability. In common with other modelling centres, the Hadley Centre model is used extensively for climate prediction studies. One of the largest uncertainties associated with such studies is the magnitude and role of cloud feedbacks. Through careful evaluation of the present-day cloud distribution and its variability, we aim to improve the model's physical parametrizations so that we can have greater confidence in our predictions of future climate.

In the following section, we describe the Hadley Centre climate model and the observational data sets used. In Section 3 we present an evaluation of tropical cloud in the current version of the atmosphere-only model, HadAM3. In Section 4 we then assess the impact of new physical parametrizations on the simulations. In Section 5 we show how the information derived from these comparisons can be used to understand the model's simulation of interannual variability in the tropical Pacific. Conclusions are presented in the final section.

## 2. Model description and observational data

We begin with an evaluation of the atmosphere-only version of the Hadley Centre climate model (Version 3) known as HadAM3 and described in Pope et al. (2000). We use the standard configuration with a horizontal resolution of 2.5° latitude by 3.75° longitude, 19 vertical levels and a 30-min time-step. The 'slab' version of this model (i.e. the atmospheric model coupled to a 50-m mixed-layer ocean and sea-ice model) is referred to as HadSM3. We then examine a more recent version of the model, referred to as HadAM4 (Webb et al. 2001), which incorporates a number of major changes with respect to HadAM3: the vertical resolution in the free troposphere is increased from 19 to 30 levels; the radiative effects of non-spherical ice particles are included (Kristjánsson et al. 1999); a new mixed-phase precipitation scheme (Wilson and Ballard, 1999) is introduced which uses a prognostic equation for cloud ice and calculates exchanges between liquid, ice and water vapour using physically-based transfer terms; a scheme to treat the radiative effects of anvil cirrus associated with deep convective systems is included (Gregory, 1999); the threshold relative humidity for cloud formation within a grid box is parametrized as a function of the horizontal variability resolved by the model (Cusack et al. 1999); a vertical gradient cloud area parametrization is introduced which allows clouds to fill only part of the vertical thickness of a model layer (Webb et al. 2001); a new boundary layer mixing scheme, including an explicit entrainment parametrization is introduced (Lock, 1998; Martin et al. 2000). The new boundary layer scheme is accompanied by an increase in the boundary layer resolution, raising the total number of vertical levels to 38. HadAM4 can be considered as a development version of the Hadley Centre climate model; the physics package forms the basis of that being developed for the next generation coupled model, which has a completely new dynamical formulation.

We analyse integrations of HadAM3 and HadAM4 forced with the observed SST and sea-ice distributions. The model is evaluated through comparisons with a combination of satellite and reanalysis data sets. The satellite data are taken from the ERBE (Barkstrom, 1984; Harrison et al. 1990) and ISCCP D2 (Rossow and Schiffer, 1999) data sets; the reanalysis data from the European Centre for Medium-Range Weather Forecasting (ERA-40; Simmons and Gibson, 1999) and the National Center for Environmental Prediction (NCEP; Kalnay et al. 1996). The ERBE data are the continuous 5-yr record from the Earth Radiation Budget Satellite (ERBS). All of these data have been processed on to a regular 2.5° by 2.5° grid. In addition to the usual diagnostics for examining clouds and their radiative effects, we also include model diagnostics which are directly comparable to ISCCP cloud amounts classified according to CTP and visible optical depth (Webb et al. 2001). We use monthly mean observations and model fields over the tropical oceans (20°N to 20°S) for the 5-yr period from January 1985 to December 1989, coinciding with the availability of the ERBE data. All quantities shown are appropriately area-weighted to allow for the slightly different resolutions of the model and observations.

## 3. Evaluation of cloud and cloud radiative effects in HadAM3

### *3.1. Mean relationships with sea surface temperature*

Several previous studies (e.g. Zhang, 1993; Bony et al. 1997a) have considered the observed relationship between clouds and

SST in the tropics. As background we first consider the mean relationships between the planetary albedo ($\alpha_p$), outgoing LW radiation (OLR) and SST and examine its representation in HadAM3. These are presented in Fig. 1, which also shows the relationship between the total cloud amount and SST for the same period.

The observations show a clear separation between the warmest (>26.5°C) and coolest (<26.5°C) SSTs, in effect dividing the tropical ocean into distinct 'regimes'. Over the warmest SSTs the albedo increases and the OLR decreases with increasing SST, so that cloud with the strongest SW and LW effects (i.e. the highest and brightest cloud) is generally to be found over the highest SSTs. Over the coolest SSTs the albedo increases with decreasing SST while the OLR (which is considerably higher than it is over warm SSTs) varies very little, indicating bright but low-level cloudiness. While HadAM3 represents the basic features of these curves, there are some notable discrepancies between the model and observations over the warmest SSTs, where the albedo is underestimated and the OLR overestimated. This indicates either that there is too little cloud or that the cloud is both too dark and too low.

The cloud amount–SST relation indicates that HadAM3 underestimates the total cloud cover over the tropical oceans. While this underestimate may explain some of the discrepancies between the observed and model cloud radiative effects, it clearly is insufficient to explain the differences everywhere. A good example of this is the albedo over cool SSTs, which agrees well with observations despite the fact that the model diagnoses only around half of the observed cloud cover. The implication is that the radiative properties of cloud over these regions are in error and this is explored in subsequent sections of this paper.

These mean relationships with SST provide some initial insight into the representation of tropical cloud in HadAM3 but are certainly not sufficient to obtain useful information regarding the reliability of the parametrizations in the model. In particular, there is considerable scatter around these mean relations (as shown by error bars on the observations) which arises due to the range of dynamical conditions and cloud properties within each SST interval. In what follows we use dynamical information from reanalyses and more detailed cloud information from ISCCP (as suggested by Webb et al. 2001) to understand how, and under what dynamical conditions, the differences between the observed and simulated cloud radiative effects occur.

### *3.2. Definition of dynamical regimes*

Following Bony et al. (1997b) we use the pressure vertical velocity at 500 hPa ($\omega_{500}$) to describe the vertical motion associated with the large-scale tropical circulation. Other choices are, of course, possible; Lau et al. (1997), for example, used the 200-hPa wind divergence. In general, the 200-hPa divergence, 850-hPa convergence and 500-hPa vertical velocity in the tropics are approximately proportional and will thus produce quite similar results (Hartmann and Michelsen, 1993).

In what follows we will investigate the relationships between clouds and their radiative effects as a function of 'dynamical regime', defined in terms of SST and vertical motion. Clearly, these relationships will be influenced by that between SST and $\omega_{500}$. The vertical velocity is driven by the convection, which itself is sensitive to SST, so SST and $\omega_{500}$ cannot be said to be truly independent variables. However, as we shall demonstrate, this approach provides a useful framework for comparing the climate model with observations and for assessing the performance of model parametrizations.

Using monthly mean data for the period January 1985–December 1989 each tropical, oceanic grid box is classified according to SST and $\omega_{500}$ in intervals of 1°C and 20 hPa $d^{-1}$, respectively. Cloud and radiation budget parameters are averaged for all tropical ocean points falling within each $\omega_{500}$–SST category and the results displayed as a two-dimensional (2-D) plot in the $\omega_{500}$–SST plane. Figure 2 compares the populations of the $\omega_{500}$–SST bins derived from ERA-40 and NCEP reanalyses with those from HadAM3 and the slab model HadSM3. The shape of these distributions (i.e. the portion of the $\omega_{500}$–SST plane which is occupied) reflects the general features of the relationship between SST and vertical motion in that higher SSTs (i.e. >27°C) are associated with a wide range of vertical velocities ranging from the strongest ascent to strong descent, whereas lower SSTs (i.e. <27°C) are associated primarily with strong descent or very weak vertical motion and only rarely with (moderate) ascent.

The clearest difference between the two reanalyses (Figs 2a and b) is that NCEP does not appear to produce the very strong ascent over high SSTs seen in ERA-40. This has also been noted by Trenberth and Guillemot (1998), who showed that the Hadley circulation was weaker in the NCEP reanalyses than in the previous European Centre for Medium-Range Weather Forecasts (ECMWF) data set (ERA; Gibson et al. 1997). Bony et al. (1997b) report very little impact on their analysis using either Data Assimilation Office (DAO) or NCEP reanalyses. This might well not be the case with ERA-40 and NCEP. The choice of vertical velocity intervals is clearly important. For example, if 'strong ascent' is simply defined as $\omega_{500} < -40$ hPa $d^{-1}$ then differences between the two reanalyses might not be so apparent. The HadAM3 distribution (Fig. 2c) corresponds closely with that derived from ERA-40, suggesting that is preferable to use ERA-40 vertical motion fields for our model comparisons; it is clearly desirable that the distribution of the dynamical regimes in the model resembles that of the observations so that dynamical dependences are not introduced. The HadAM3 distribution represents the model's response to prescribed SSTs. Figure 2d implies, reassuringly, that this is representative of the model's behaviour in general, although it can be noted that the slab model does not appear to reproduce the highest SSTs. This is undoubtedly due to the use of climatological mean Q-fluxes.

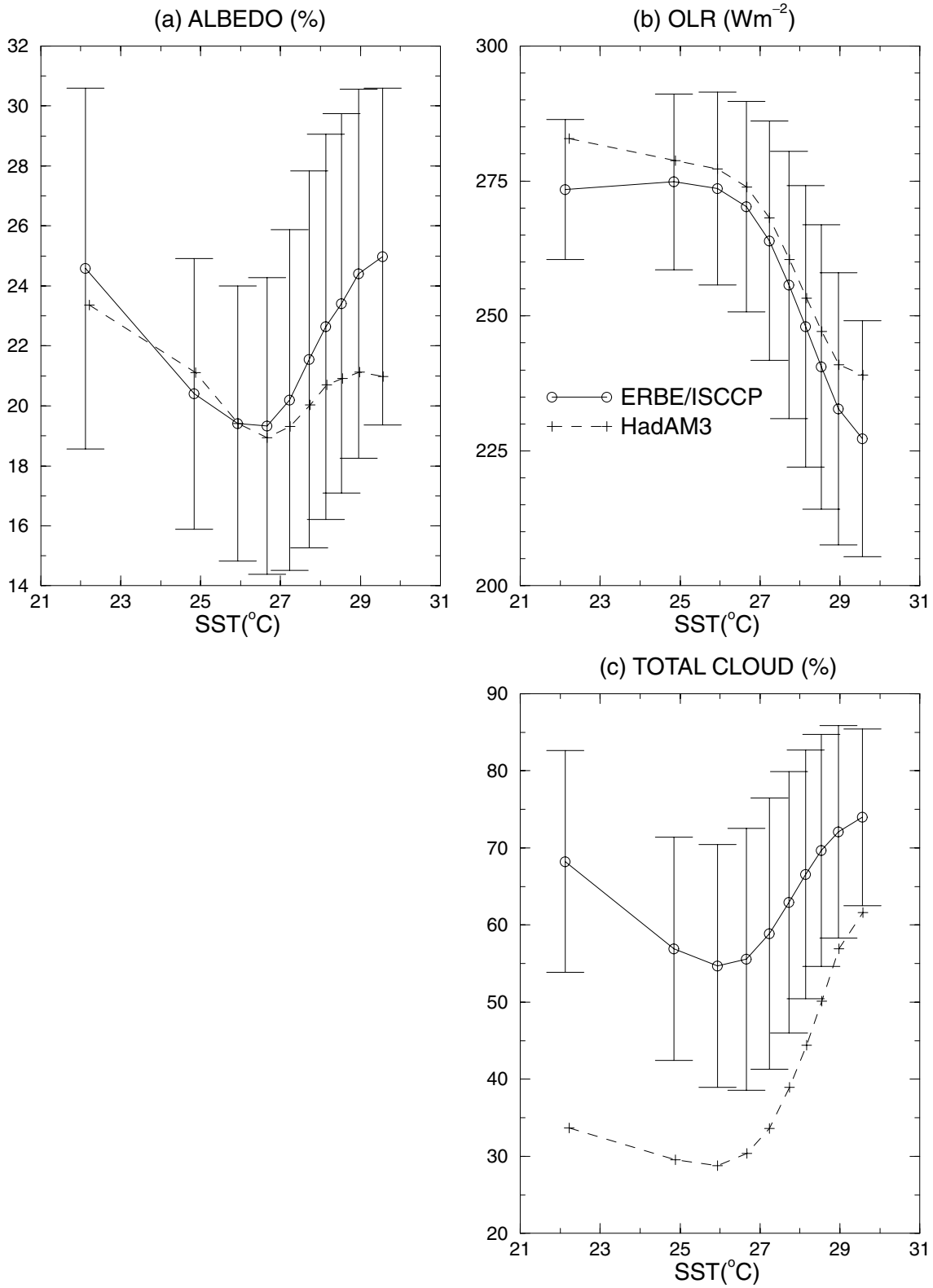


*Fig 1.* The mean relationships between SST and (a) planetary albedo, (b) OLR and (c) total cloud amount derived from observations and HadAM3 over the tropical oceans for the period 1985–89. Quantities are averaged over deciles of SST so that each interval contains the same number of points. The error bars shown on the observations represent ±1 standard deviation about the mean values.

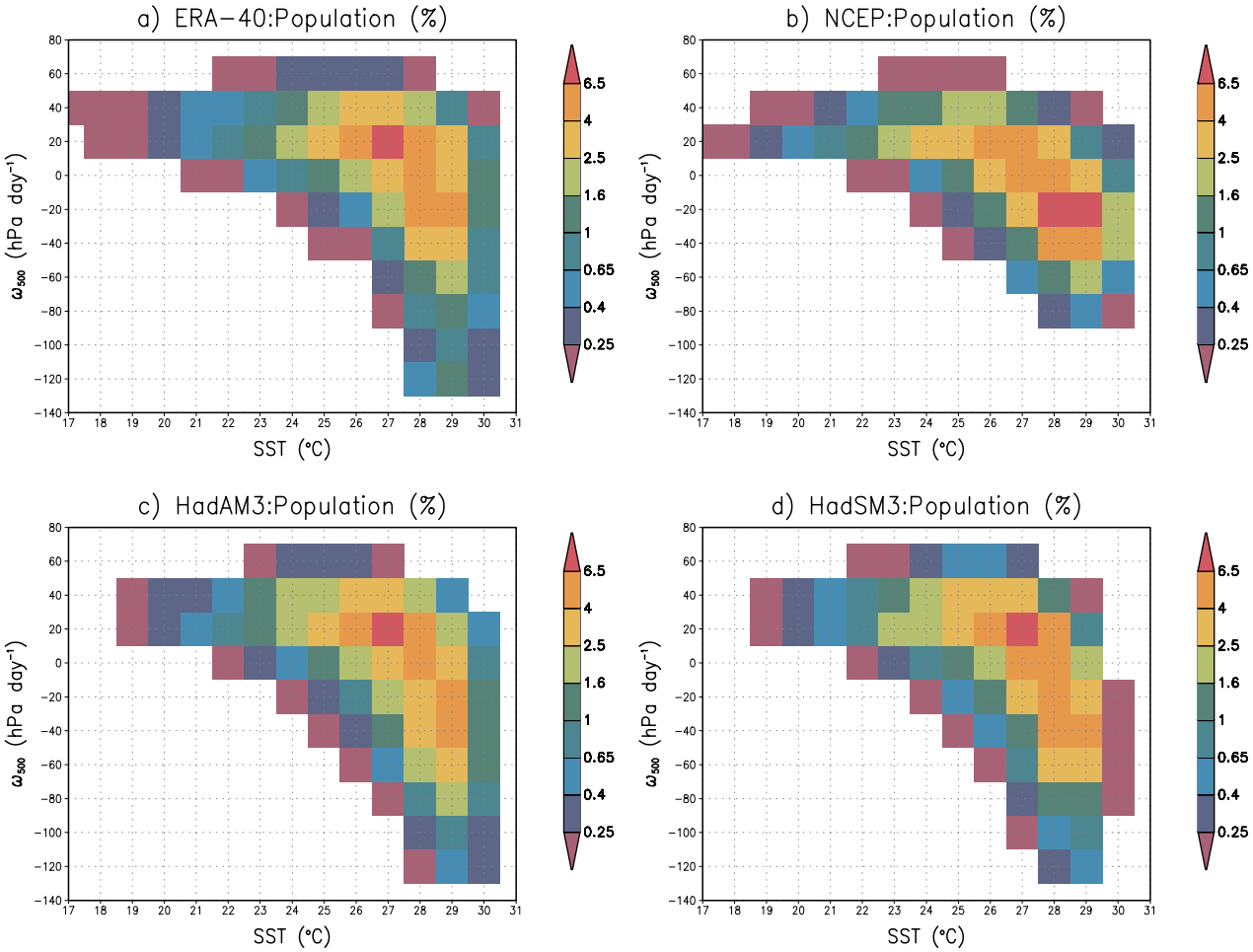


*Fig 2.* The populations of the $\omega_{500}$–SST bins derived from (a) ECMWF reanalyses (ERA), (b) NCEP reanalyses, (c) HadAM3 forced with observed SSTs and (d) HadSM3, the 'slab' model. Values shown are percentages of the total number of points over the tropical oceans. The scale is logarithmic with an interval of $\log_{10}(\text{population}) = 0.2$.

### *3.3. Albedo, OLR and total cloud amount*

Figure 3 shows $\omega_{500}$–SST plots of $\alpha_p$, OLR and total cloud amount, quantities that were examined with respect to SST only in Fig. 1. A comparison is shown between observations (using a combination of ERBE or ISCCP data, ERA-40 vertical motion and observed SST) and HadAM3 forced with observed SSTs. To ensure a reliable statistical sample, values are shown only for those bins containing at least 100 points.

We consider the albedo and OLR observations first (Figs 3a and c). The highest values of $\alpha_p$ are found over the two extremes of the $\omega_{500}$–SST distribution: strong ascent ($\omega_{500} < 0$) over the warmest SSTs and strong descent ($\omega_{500} > 0$) over the coolest waters. $\alpha_p$ clearly increases with greater ascent for SSTs in excess of 25°C, although this increase is also discernable for SSTs greater than 22°C. Over the warm SSTs there is a decrease of $\alpha_p$ with enhanced descending motion, so that the lowest values of $\alpha_p$ are found over the warmest waters. Over descent regions $\alpha_p$ generally increases with decreasing SST. This contrasts with areas of ascent, where there is very little dependence of $\alpha_p$ with SST, although it should be noted that the SST range is much smaller.

Over warm SSTs the OLR decreases with both strengthened ascent and increased SST. Over cooler SSTs the situation is different. Here, the highest values of OLR are found and there is very little dependence on SST. Taken together these two figures summarize the basic features of the relationship between clouds, SST and the large-scale circulation over the tropical oceans. Over the warmest waters a range of dynamical conditions exist ranging from strong ascent (where there is high, bright cloud associated with convection, which has strong effects in both the SW and LW) to strong descent (where there is little high cloud, convection is suppressed and there is only a small cloud effect in both the SW and LW). The wide range of both $\alpha_p$ and OLR over the warmest waters corresponds to the wide range of $\omega_{500}$ and helps to explain a large part of the variation of $\alpha_p$ and OLR at these SSTs seen in Fig. 1. Over the coolest waters, the SW radiative effect clearly increases with decreasing SST, while showing only a

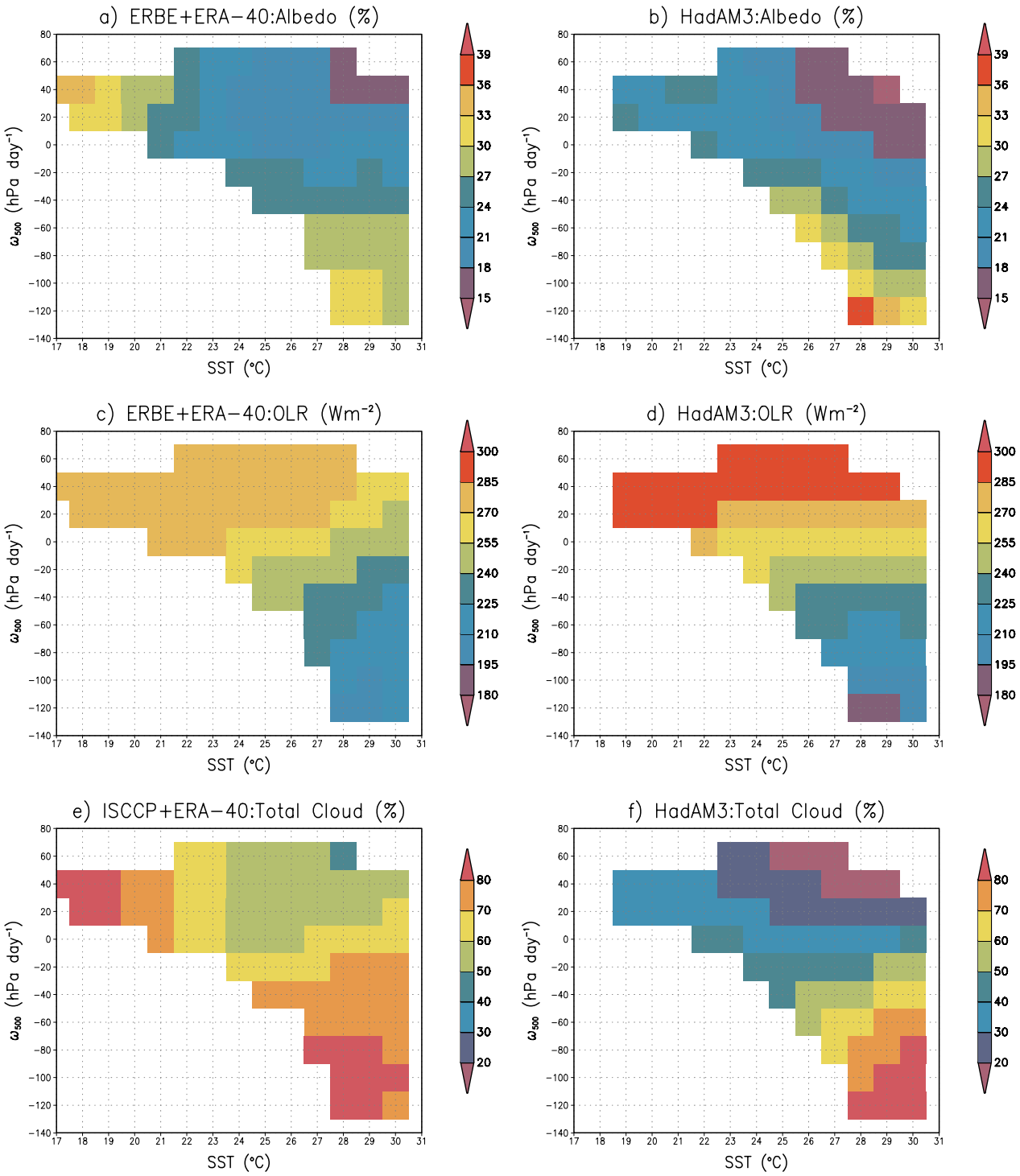


*Fig 3.* Mean $\omega_{500}$–SST distributions of (a), (b) observed and HadAM3 albedo, (c), (d) observed and HadAM3 OLR, and (e), (f) observed and HadAM3 total cloud amount.

weak dependence on the vertical motion, whereas the LW effect is weak and shows little dependence on either SST or $\omega_{500}$. This corresponds to increasing low-level cloud with decreasing SST over regions of descending motion. Over the coolest waters, the much narrower range of $\omega_{500}$ is clearly not sufficient to explain the wide variation of albedo seen in Fig. 1. In this case the variation arises due to a wide range of either cloud amount or cloud optical properties within these regions.

The HadAM3 simulation (Figs 3b and d) shows that the model captures the basic features seen in the observations: the highest $\alpha_p$ and lowest OLR values are found over strong ascent/warm SST; relatively high $\alpha_p$ and high OLR are found over strong descent/cool SST; low $\alpha_p$ and high OLR are seen over warm SST/descent. However, there are important differences. First, there is a clear tendency for $\alpha_p$ to decrease with increasing SST in regions of strong ascent. This rather curious result comes about partly because the highest albedos are actually found over the South Pacific Convergence Zone, away from the warmest waters of the warm pool, and might also be due to the intrusion of systems from higher latitudes into the region of study. Secondly, the albedo in areas of strongest descent over cool SSTs is considerably lower than that observed. The principal difference between the observed and HadAM3 OLR distributions is the model's inability to reproduce the observed decrease of OLR with increasing SST along lines of constant $\omega_{500}$. This is particularly apparent over the warmest waters.

Now consider the total cloud amount distributions (Figs 3e and f). The observations illustrate the important first-order dependence of the albedo on the total cloud amount and also show the increase of high-level cloud with increasing ascent over warm SSTs, corresponding to the increase in $\alpha_p$ and the decrease in OLR. Note that in areas of strongest descent over warm SSTs, where ERBE indicates both low albedos and high OLR, the ISCCP data still suggest cloud amounts in excess of 50%. Examination of the ISCCP cloud type data (not shown) suggests this is mainly high, optically thin cloud. Aside from areas of warm SST and strong ascent, HadAM3 underestimates total cloud amount compared to ISCCP. In areas of cool SST and descent this underestimate of cloud corresponds to values of albedo which, while underestimated by the model, are perhaps not as low as the cloud discrepancy might suggest. In the areas of strongest ascent over warm SSTs the model simulation indicates cloud amounts comparable to ISCCP. The implication is that the cloud properties are misrepresented in the model. For example, it appears that low-level cloud over cool SST descent is too bright so that even with cloud amounts less than half of those observed the model is able to produce a fairly reasonable simulation of the albedo. In the following section, more detailed ISCCP data are used to investigate this further.

Two further points need to be made regarding these distributions. First, the distributions are robust; removing data from any particular year, including the ENSO year of 1987, leaves the albedo and OLR distributions essentially unchanged. When the distributions are derived separately for the different ocean basins they again differ very little, the only noteworthy change being the removal of the highest albedo and lowest OLR values over strong ascent when the Pacific Ocean is excluded from the analysis. Secondly, we have chosen to look at $\alpha_p$ and OLR rather than cloud radiative forcing diagnostics as this avoids problems due to inconsistent sampling between the model and observed clear-sky fluxes (Cess and Potter, 1987). These are particularly apparent in areas of strong ascent over the warmest SSTs, where the biases in the clear-sky OLR can be up to 15 W m$^{-2}$. Such biases will obviously tend to obscure meaningful comparisons between the model and observed cloud forcing fields (Allan and Ringer, 2003).

### *3.4. Comparisons with ISCCP cloud diagnostics*

It can be seen from the above comparisons that, in general, differences in the total cloud amount alone are not sufficient to explain those in the radiative effects of clouds between the climate model simulations and the observations. It is therefore necessary to consider the cloud properties in more detail. This can be achieved through comparisons of ISCCP data, which classify cloud types according to CTP and visible optical depth ($\tau_{vis}$), with corresponding diagnostics derived from the climate model (see Webb et al. 2001). Figure 4 shows $\omega_{500}$–SST plots of high cloud types (defined as cloud with CTP <440 hPa) and again compares observations with HadAM3. The observations show the close correspondence between the OLR and high cloud amount distributions (Figs 4a and 3c). The high albedos over the warmest SSTs are also seen to be associated with large amounts of high cloud.

The distribution of high cloud amount as a function of regime is generally well represented in HadAM3 (Fig. 4b), although it appears to be overestimated in areas of strong ascent over the warmest SSTs. However, as was the case with total cloud amount, it can be seen that the total high cloud distributions alone cannot explain the differences between the model and observed distributions of albedo and OLR. The variation of high cloud with both SST and $\omega_{500}$ is simulated well in the model, but Fig. 3 demonstrates that this is not the case for the albedo and OLR. As one moves to the areas of warmest SSTs and strongest ascending motion, for example, the observations imply that high cloud amount increases and this is associated with corresponding increases in $\alpha_p$ and decreases in OLR. Although these increases in high cloud are realistic in HadAM3 the variation of both of $\alpha_p$ and OLR is clearly less so; there is little if no variation of OLR with SST and $\alpha_p$ actually decreases as both SST and the strength of the ascent increase. Looking at the ISCCP data in further detail, Figs 4c–f show the observed and model distributions of high cloud with $3.6 < \tau_{vis} < 23$ and $\tau_{vis} > 23$. These imply that, over warm SSTs in areas of strongest ascent, HadAM3 overestimates the amount of high, optically thick cloud. Moreover, this optically thick cloud shows a decreasing relationship with SST. This explains the inverse relationship of $\alpha_p$ to SST in the model. Taken together, the ERBE radiation budget and ISCCP high cloud distributions imply that it is the ensemble of cloud types with varying optical thickness that ultimately determines the overall radiative effect in both the SW and LW (Hartmann et al. 2001). Figure 4 indicates that it is a failure to represent the correct amounts of different cloud types in this ensemble that leads to the errors in the radiative effects seen in HadAM3. In particular, HadAM3 underestimates high cloud of 'intermediate'

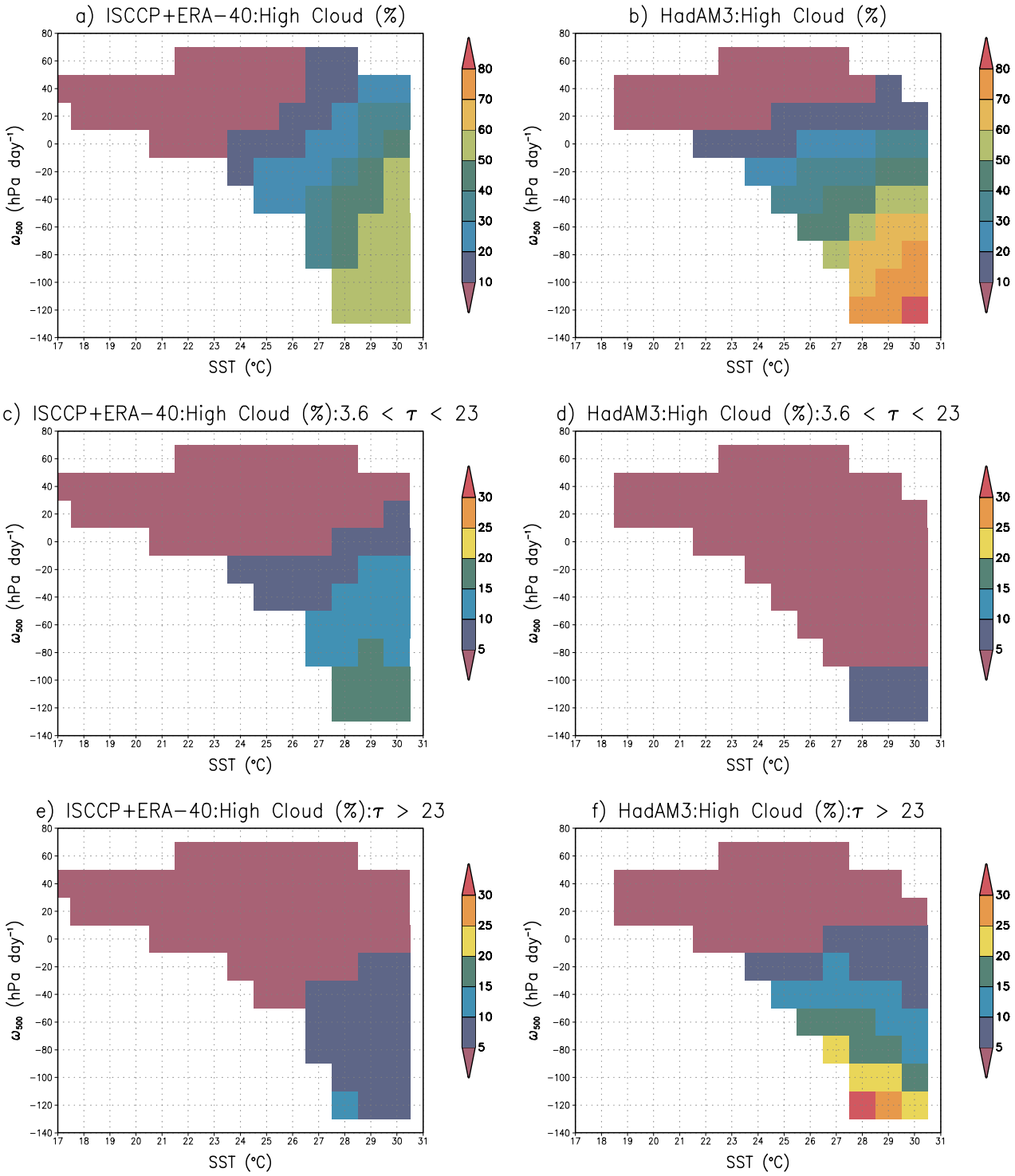


*Fig 4.* As Fig. 3 but for (a), (b) total high cloud amount, (c), (d) high cloud with $3.6 < \tau_{vis} < 23$ and (e), (f) high cloud with $\tau_{vis} > 23$.

optical thickness (i.e. $3.6 < \tau_{vis} < 23$) and overestimates the amount of the optically thickest cloud ($\tau_{vis} > 23$). This can be explained by considering the calculation of convective cloud amount in the model. In HadAM3, the convective cloud fraction is diagnosed empirically from a linear relation with the logarithm of total water flux. This cloud fraction is not permitted to vary with height within a model grid box and is applied as a constant value between the diagnosed ensemble cloud base and top. The

scheme typically produces convective cloud amounts of $\sim 1/3$, which is an overestimate for deep convective towers alone but an underestimate of typical anvil cloud fractions. (It may also be noted that the scheme is likely to provide unrealistic radiative heating profiles.) It is thus an inability to represent the convective anvils correctly that leads to the underestimate of high cloud with intermediate optical thickness. The overestimate of the optically thickest high cloud is also the result of excessive cloud water contents. This is explored further in the following section, where the impact of including a relatively simple parametrization for the anvils is discussed.

Figure 5 shows similar plots to those of Fig. 4 for ISCCP low cloud types, defined as cloud with CTP $>680$ hPa. Figures 5a and b confirm that the underestimate of total cloud amount in areas of cooler SSTs and descent is primarily a result of the underestimate of low-level cloud in these areas. It can also be seen that the apparently reasonable simulation of $\alpha_p$ in these areas, which is incompatible with the underestimate of low and total cloud amount, is in fact due to an overestimate of the optically thickest low-level cloud (Figs 5e and f). Once again, the importance of correctly simulating both the cloud amounts and the cloud properties is highlighted. The underestimate in low-level cloud, which also results from a lack of optically thin cloud ($\tau_{vis} < 3.6$), can be attributed to the poor vertical resolution in the lower troposphere, an incorrect representation of boundary layer mixing in these conditions and also to the fact that the model does not represent entrainment (Bushell and Martin, 1999; Martin et al. 2000). The impact of a new boundary layer mixing scheme, which includes an explicit parametrization for entrainment, is discussed in the following section.

## 4. Assessing the impact of new physical parametrizations

### *4.1. Comparison of HadAM3 and HadAM4*

In this section we apply the above methodology to look at the impact of some of the parametrization changes between different versions of the Hadley Centre climate model. First, we look at the differences between HadAM3 and a version of the model, known as HadAM4, containing several important changes to the model's physical parametrizations, as described in Section 2. We then consider the impact of two of these parametrizations in more detail: the representation of the radiative effects of convective anvils (Gregory, 1999) and the new boundary layer mixing scheme (Lock, 1998; Martin et al. 2000).

Figure 6 shows $\omega_{500}$–SST plots of $\alpha_p$, OLR and total cloud amount distributions for HadAM4, together with differences between HadAM4 and HadAM3. These are again constructed from monthly mean data for the period 1985–89, with the model being forced by observed SSTs and sea ice. Aside from areas of warm SST and strong ascent, HadAM4 still underestimates the total cloud amount compared to ISCCP, although the cloud amount has generally been increased compared to HadAM3. The comparisons between HadAM3 and HadAM4 are particularly interesting in areas of ascent over warm SSTs; although the dependence of cloud amount on SST and $\omega_{500}$ is similar in the two models, there is clearly greater consistency (i.e. the observed first-order relationships are better simulated) between the cloud amount and both the $\alpha_p$ and OLR distributions in HadAM4. It is also worth noting that, although the cloud amount in these areas is comparable in the two models, $\alpha_p$ is higher and OLR lower in HadAM4. However, the decrease of $\alpha_p$ with increasing SST has been eliminated and the dependence of OLR on SST has been improved. These changes are clearly seen in the difference plots, which again emphasize the limited value of considering total cloud amount alone. In areas of cool SST/descent cloud amount increases but the albedo decreases, while in areas of warm SST/ascent the increased albedo and reduced OLR indicate stronger cloud radiative effects in the both the SW and LW even though the cloud amount is slightly reduced.

Figure 7 shows the distributions of ISCCP high and low cloud types for HadAM4. As with HadAM3 the distribution of high cloud amount as a function of regime is well represented in this version of the model, with cloud amount again being overestimated in areas of strong ascent over the warmest SSTs. More importantly, the distribution of high cloud is now seen to be consistent with those of $\alpha_p$ and OLR in HadAM4 in a manner similar to that seen between the ERBE and ISCCP data. It can also be seen that high cloud of intermediate optical thickness has been increased, although it is clear that this cloud type and the optically thickest high cloud ($\tau_{vis} > 23$) are both overestimated, which leads to the excessive albedo values. The total low-level cloud amount is, similarly to HadAM3, underestimated in regions of descent over cooler SSTs. It can be seen, however, that the excessive amount of the optically thickest low cloud has mostly been removed, so it is now primarily the underestimate in the total amount of low cloud that leads to the underestimated albedo.

We next focus on two of the changes that have the largest impact on the simulation of clouds and the radiation budget in the tropics: the convective anvil parametrization and the new boundary layer mixing scheme. These two parametrizations also have important impacts on climate change simulations with the Hadley Centre model (Williams et al. 2003).

### *4.2. Impact of the convective anvil parametrization*

It should first be noted that the anvil parametrization (Gregory, 1999) seeks only to represent the radiative effect of the convective anvils; no attempt is made to represent either their thermodynamic or microphysical impacts. The anvil scheme attempts to incorporate some basic observational facts regarding anvil cloud: they are associated with deep convection; they are composed of ice particles; and they have their base at the freezing level. The convective cloud amount is modified when deep convection

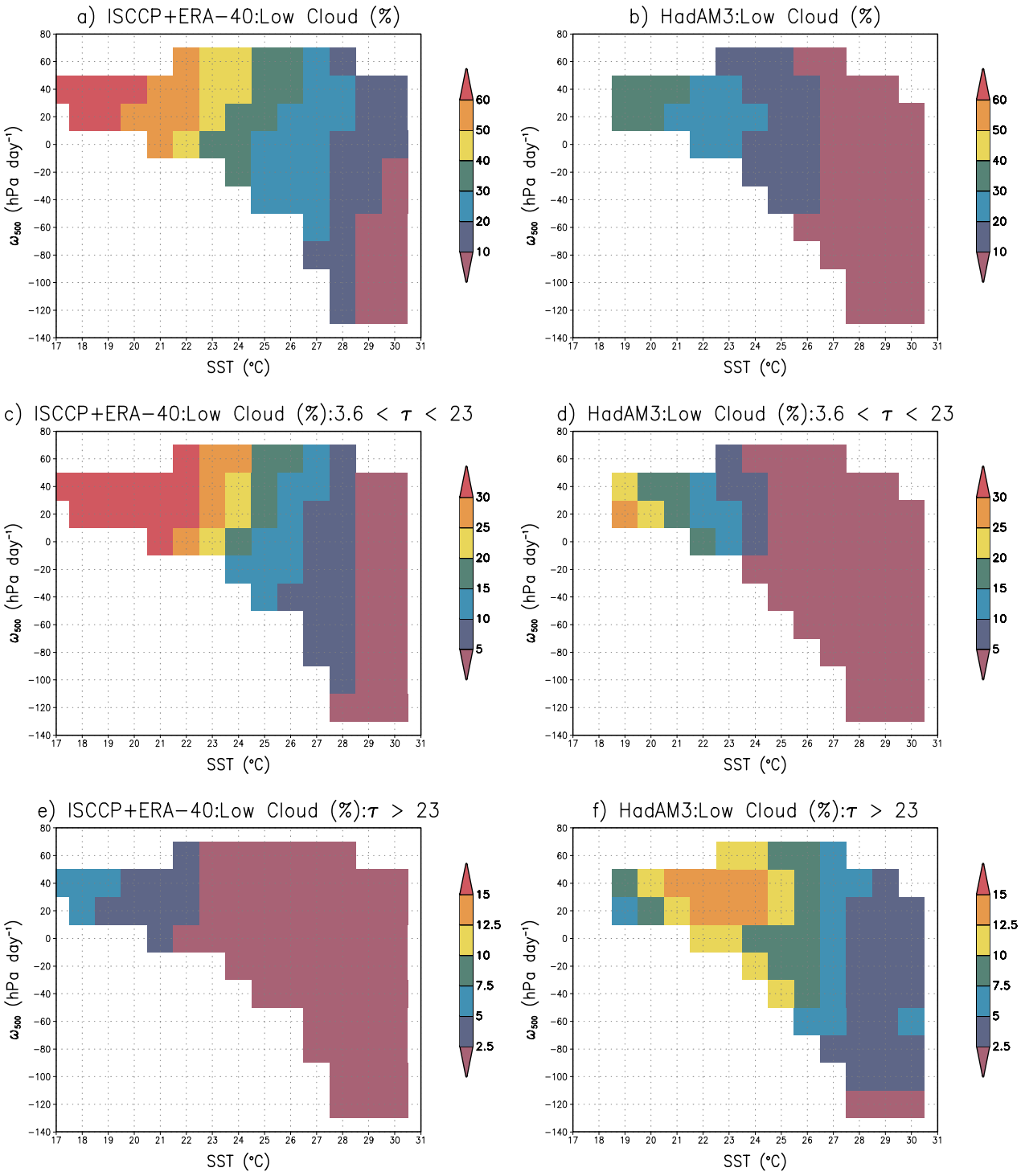


*Fig 5*. As Fig. 4 but for low cloud.

occurs; the cloud fraction is increased linearly with height above the freezing level to the cloud top (this represents the anvil) and decreased to a constant value below the freezing level (representing the convective tower). It is this revised convective cloud fraction which is passed to the radiation scheme. Deep convective clouds are defined as having their bases in the boundary layer and tops above the freezing level. The issue of excessive convective cloud water is addressed in two ways. First, convective precipitation is now excluded from the water path 'seen' by the radiation scheme. Secondly, an 'updraught factor' is introduced

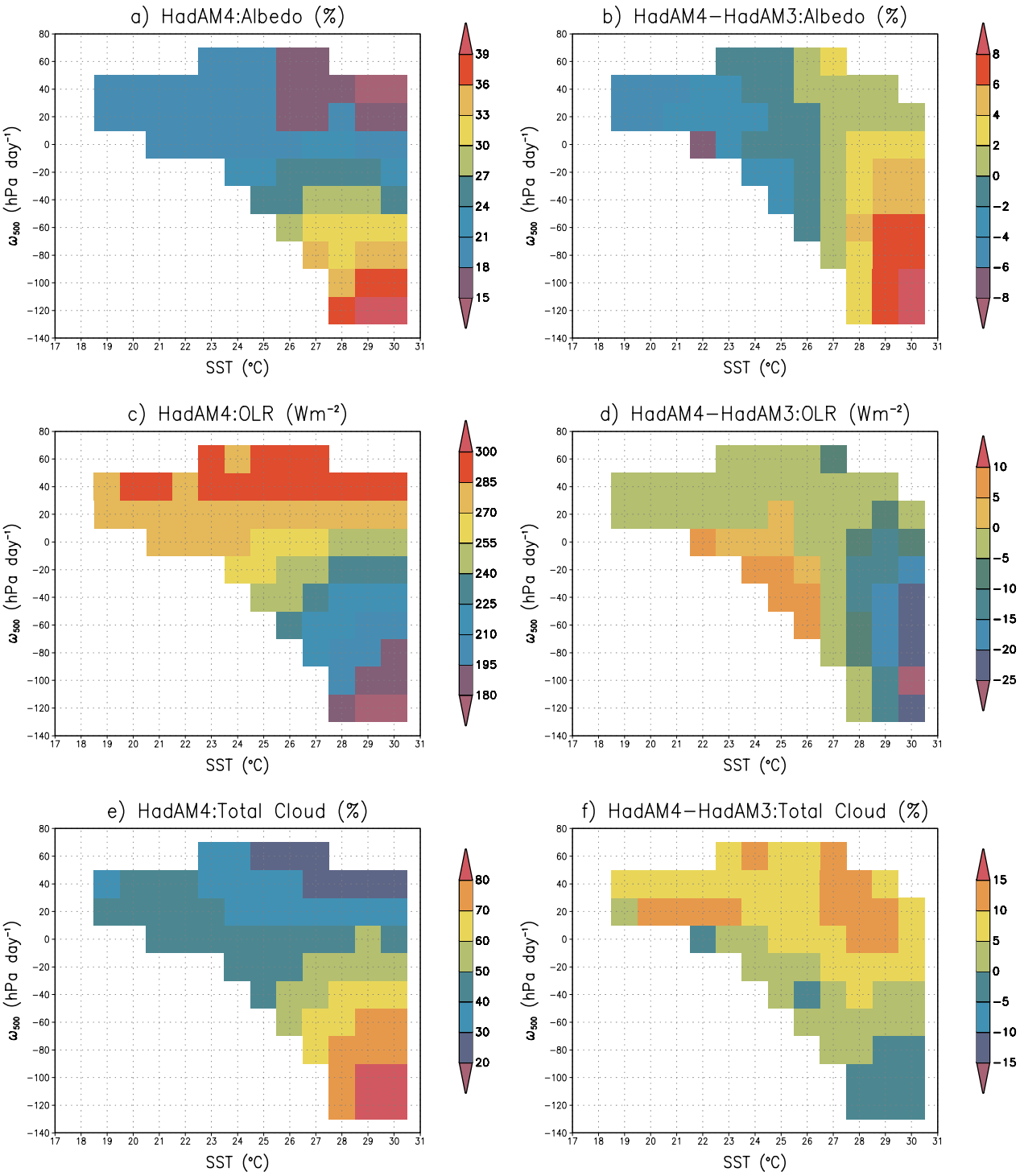


*Fig 6.* Mean $\omega_{500}$–SST distributions of (a) albedo, (c) OLR and (e) total cloud amount for HadAM4. Mean distributions of the differences between HadAM4 and HadAM3 of (b) albedo, (d) OLR and (f) total cloud amount.

which seeks to reduce convective cloud water while not directly altering convection.

We recognize that this parametrization, and the introduction of these factors, is highly empirical and likely to be very model specific; the primary objective here is to demonstrate how its effects can be assessed within the dynamical regimes framework. However, it should also be noted that the anvil scheme produces more realistic heating rate profiles than HadAM3 (Gregory, 1999) and

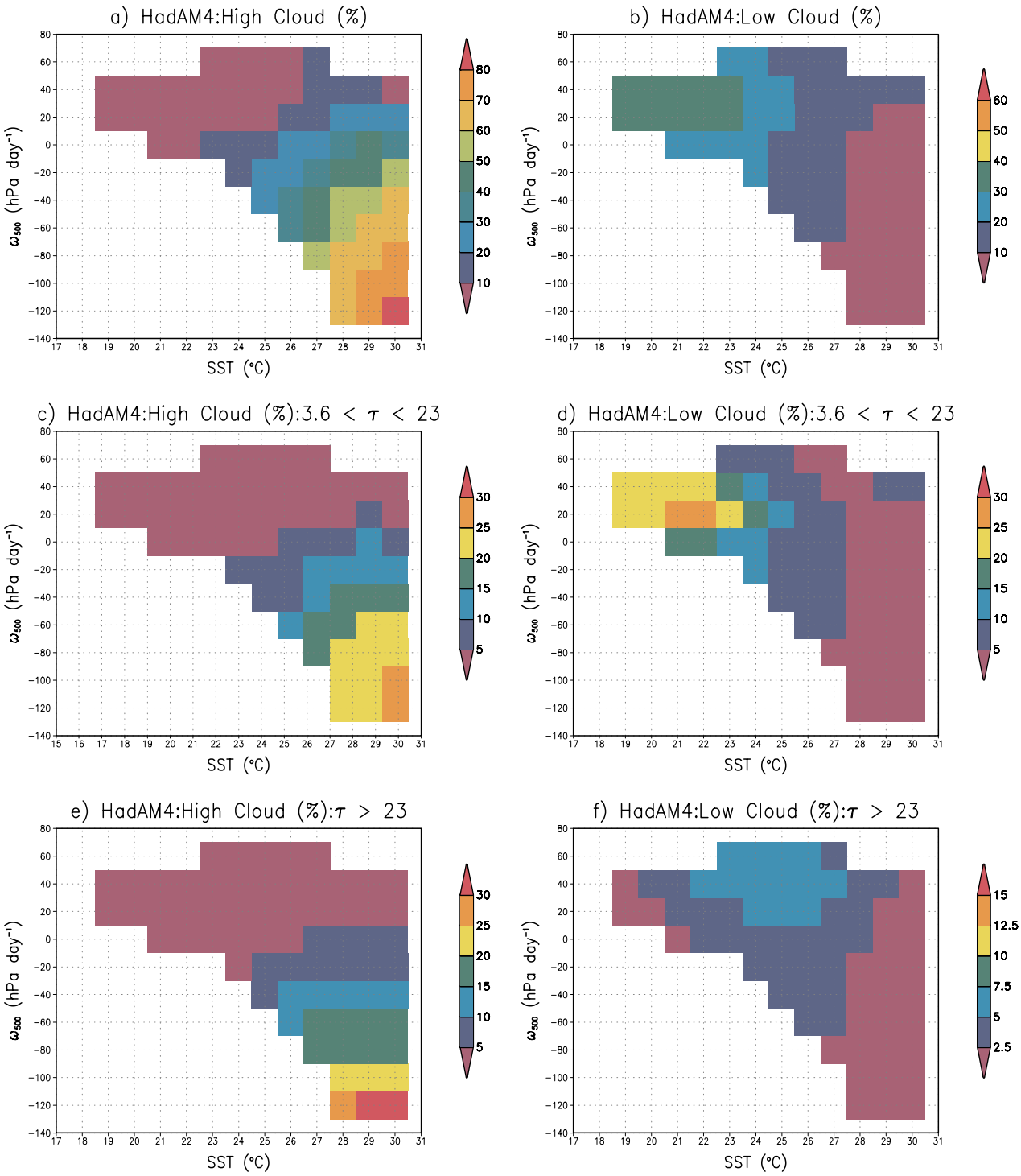


*Fig 7.* Mean $\omega_{500}$–SST distributions for HadAM4 of (a), (c) and (e) high cloud and (b), (d) and (f) low cloud amounts.

also results in an improved simulation of the observed correlation between the high/thick and high/intermediate cloud (Chou and Neelin, 1999) in the model. Considering all tropical ocean points over the 1985–89 period the observed linear correlation coefficient between these cloud types is 0.85, in HadAM3 it is 0.52, in HadAM4 it is 0.84, and in HadAM4 with the anvil scheme removed it is 0.62.

Figure 8 shows the albedo, OLR, and high, intermediate and optically thick cloud distributions for HadAM4 when the anvil parametrization has been removed. The effects are, of course,

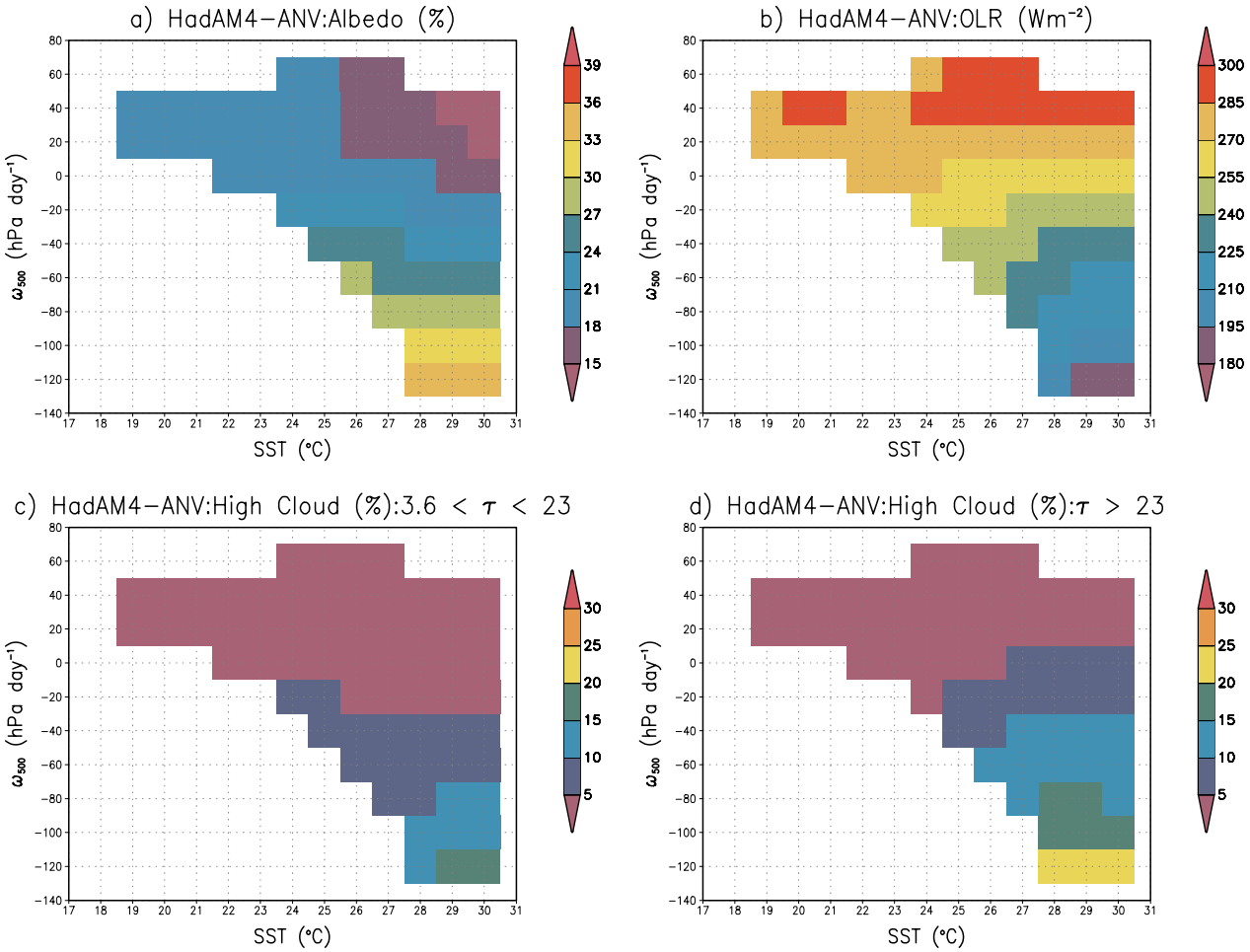


*Fig 8.* Mean $\omega_{500}$–SST distributions of (a) albedo, (b) OLR, (c) high cloud with $3.6 < \tau_{vis} < 23$ and (d) high cloud with $\tau_{vis} > 23$ for HadAM4 with the convective anvil parametrization removed.

largely restricted to areas of ascent over the warmest SSTs. Clearly, the greatest impact is the reduction of high, intermediate optical thickness cloud (compare Fig. 8c with Fig. 7c) which leads to a reduction in the albedo and an increase in the OLR. There is also a reduction in the optically thickest high cloud, although, as was the case with HadAM3, this still remains excessive compared to observations. This analysis shows the effects of the anvil scheme to be somewhat ambiguous. While it clearly has the desired effect of introducing the high, intermediate thickness cloud lacking in HadAM3, its effects on both the albedo and OLR appear to be excessive.

Zender and Kiehl (1997) examined the sensitivity of the National Center for Atmospheric Research (NCAR) Community Climate Model to a more sophisticated prognostic anvil scheme which incorporated a number of observed microphysical characteristics of anvils: enhanced ice content in the anvil; the observed vertical distribution of condensate; and the link between cloud base mass flux and anvil growth rate. Interestingly, they found little impact on the top-of-atmosphere cloud radiative effects despite twofold to fourfold increases in anvil mass. The effects of increased ice amount and fraction were approximately compensated by reduced extinction per unit mass due to the vertical location of the anvil being tied to larger hydrometeor size. Clearly, refinements to the scheme used here are desirable, both for more accurate present-day simulations and reliable climate change predictions. The radiative forcing from tropical anvils plays a major role in determining the diabatic heating which drives the large-scale circulation. Furthermore, both Yao and Del Genio (1999), using the Goddard Institute for Space Studies GCM, and Williams et al. (2003), using the present anvil parametrization in slab model versions of the Hadley Centre model, have shown that anvil clouds have the potential to significantly alter the climate sensitivity to a doubling of $CO_2$.

### *4.3. Impact of the new boundary layer scheme*

The new boundary layer scheme identifies different mixing regimes leading to the classification of six different boundary

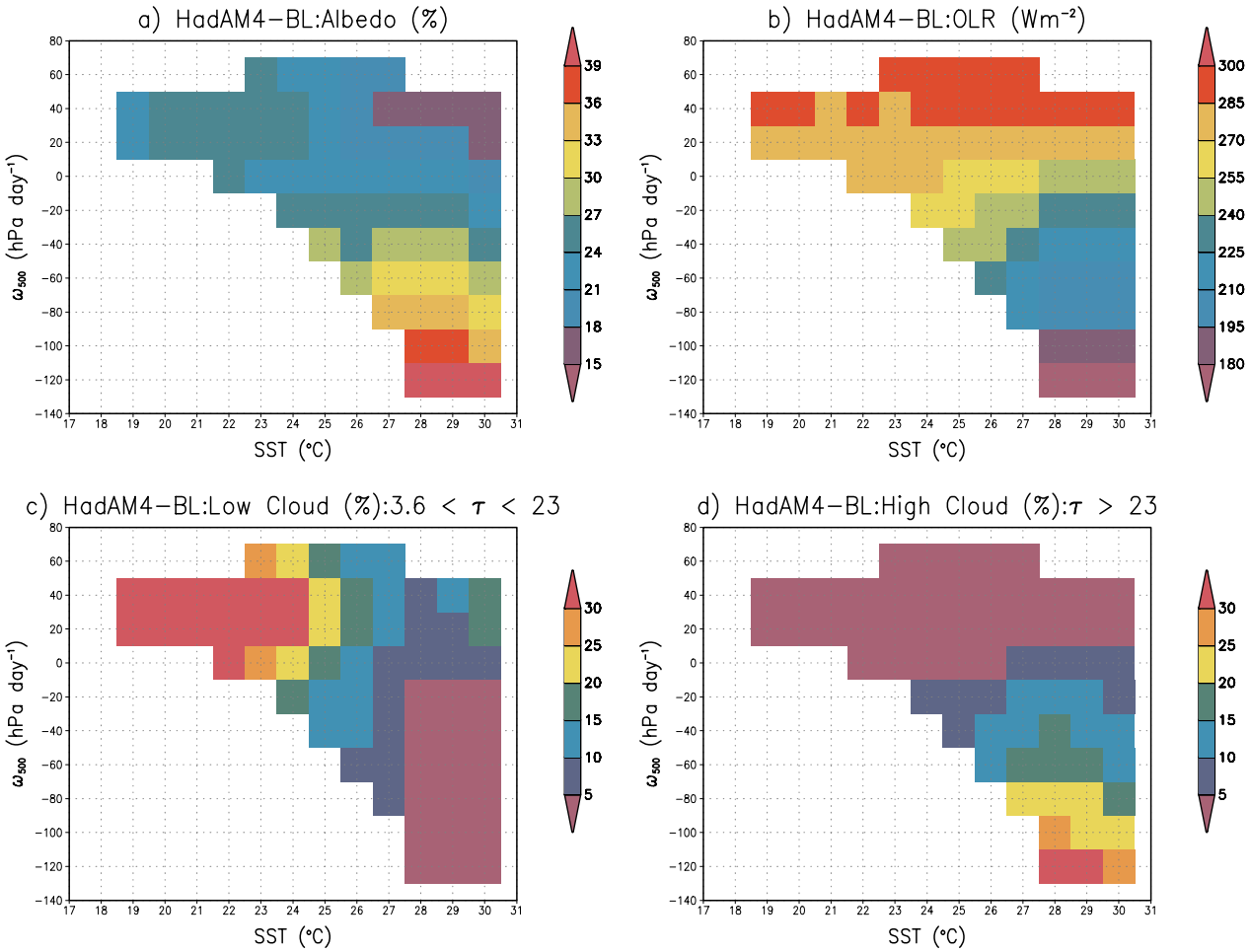


*Fig 9.* Mean $\omega_{500}$–SST distributions of (a) albedo, (b) OLR, (c) low cloud with $3.6 < \tau_{\mathrm{vis}} < 23$ and (d) high cloud with $\tau_{\mathrm{vis}} > 23$ for HadAM4 with the new boundary layer mixing scheme removed.

layer types: stable (types I and II); well mixed (types III and IV); and cumulus capped (types V and VI). The full details of the scheme and its performance in single-column model tests are given in Lock et al. (2000), with tests of its implementation in HadAM3 and the mesoscale forecasting version of the Unified Model being described in Martin et al. (2000). At each model time-step, a grid point is classified as falling into one of these six boundary layer types. The fractional occurrence of the different types, if desired, can be obtained by averaging over the required time interval.

Figure 9 shows the albedo and OLR distributions, together with those of low cloud with $3.6 < \tau_{\mathrm{vis}} < 23$ and high cloud with $\tau_{\mathrm{vis}} > 23$ for HadAM4 with the new boundary layer scheme removed. Removal of the scheme results in an increase in intermediate thickness low cloud in regions of descent, with an associated increase in the albedo. There is also a slight reduction in the optically thickest low cloud. Comparisons with Figs 7 and 5 imply that removing the boundary scheme is not clearly detrimental to the simulation of cloud in the descent regions. However, it is known that the scheme produces much more physically realistic boundary layer types—both the structure of the boundary layer and the representation of mixing processes are improved—when compared to observations (see Martin et al. 2000, for details). Martin et al. (2000) tested the new scheme in HadAM3 and found that it actually resulted in less cloud in the stratocumulus regions—areas where the model already produced too little cloud in the first place. It thus appears that the ability of both HadAM3 and HadAM4 to make use of the scheme (certainly in terms of generating cloud) is limited by other, more fundamental, aspects of the model. Indeed, initial analysis of a development version of the new Hadley Centre climate model, which includes the new boundary layer scheme and uses a semi-Lagrangian dynamical formulation and a different vertical grid, indicates that much more realistic cloud amounts and cloud radiative effects are achieved in these areas of large-scale descent.

In areas of strong ascent over warm SST, the removal of the scheme leads to the reappearance of the inverse relationship of albedo with increasing SST seen in HadAM3 (cf. Fig. 3b) and also leads to a weaker dependence of the OLR on SST. This is related to the simulation of deep convective cloud (Fig. 9d),

which shows a similar inverse dependence on SST to the albedo when the boundary layer scheme is removed. Clearly, the representation of the boundary layer—which would in this case be classified by the scheme as 'unstable, cumulus capped' (see Lock et al. 2000)—is also relevant to simulations in these regions. The improvements probably arise as a result of the combination of the new mixing scheme (and the inclusion of entrainment) with the increased boundary layer resolution which aids the formation of deeper boundary layers and improves the interaction of the boundary layer with the free troposphere.

## 5. Interannual variability in the tropical Pacific Ocean

In this section we consider how the relationships between clouds, cloud radiative effects and dynamics influence the model's simulation of the interannual variability in the tropical Pacific during the period 1985–89. The interannual variations during this period are dominated by the El Niño warm event of 1986–87 and the subsequent cold La Niña event of 1988 (e.g. Kousky, 1989; Kousky and Leetmaa, 1989). The large perturbations to the radiation budget and clouds associated with the maximum warming, which occurred around April 1987, were reported by Chou (1994).

Figure 10 shows the evolution of the anomalies in reflected SW radiation (RSW) and OLR across the equatorial Pacific for the period 1985–89. The observed ERBE anomalies are shown together with those from simulations of HadAM3 and HadAM4 forced with observed SSTs. The perturbations to the clouds and radiation budget are, of course, related to the variations in SST and the associated changes to the circulation. The observed large RSW and OLR anomalies during 1987 (Figs 10a and b) are related to the SST warming and the associated eastward migration of convection across the Pacific. The corresponding increase in latent heat released in this area resulted in a strengthened Hadley circulation, transporting more energy away from the equatorial region (Oort and Yienger, 1996; Sun and Trenberth, 1998). Both HadAM3 and HadAM4 are able to reproduce these circulation changes well; Fig. 11 compares the evolution of the 500-hPa vertical velocity anomalies over the equatorial Pacific from HadAM3 and HadAM4 with those derived from ERA-40 and NCEP. This shows the close correspondence of the reanalysis vertical motion anomalies, particularly those from ERA-40, to those in the radiation budget and cloud (Figs 10 and 12). It is also apparent that the vertical velocity anomalies from both versions of the model much more closely resemble those from ERA-40 than from NCEP. This suggests that any deficiencies in the simulations of the radiation budget and cloud anomalies arise primarily due to weaknesses in the models' physical parametrizations and also that differences between the two versions of the model are largely due to changes in these parametrizations, as discussed in previous sections.

Returning to Fig. 10, the positive RSW anomalies (i.e. cooling) and negative OLR anomalies (warming) during 1986–87 over 160°E to 160°W are well reproduced by HadAM3, although they are slightly too weak in both cases; the negative RSW anomalies (warming) and positive OLR anomalies (cooling) during late 1988/early 1989 are both weaker than observed. In contrast, both the RSW and OLR anomalies in HadAM4 compare much better with ERBE, although in both cases the anomalies are larger and more extensive than observed, whether related to either warmer (1987) or cooler (1988) than normal SSTs.

Figure 12 compares the evolution of anomalies in the intermediate thickness and optically thickest high cloud from the ISCCP observations with the HadAM3 and HadAM4 AMIP simulations. The observations indicate how the most important RSW and OLR anomalies are closely linked to the variations in these cloud types. The inability of HadAM3 to simulate high, intermediate thickness cloud leads to inconsistencies between the simulated cloud and radiation budget anomalies. During the 1987 El Niño, the overestimate of the optically thickest high cloud acts to compensate for this deficiency so that the RSW and OLR anomalies are reasonably well simulated. This is not so, however, for the La Niña event the following year; in this case, the failure to simulate the, albeit smaller, anomalies in high, intermediate thickness cloud leads to the underestimate of those in the RSW and OLR. During the El Niño warming period, SSTs increase sufficiently to allow convection to develop in areas where it normally does not occur. This also happens in HadAM3 forced with observed SSTs; in this case, the model's tendency to produce too much deep convective cloud ($\tau_{vis} > 23$) in areas of strong ascent over warm SSTs acts to compensate for the lack of intermediate thickness high cloud and a reasonable simulation of the RSW and OLR anomalies results. During the period of cooler than normal SSTs in 1988 no such compensatory mechanism is possible, resulting in a much less realistic simulation of the radiation budget anomalies.

The HadAM4 simulations show that overestimates in both of these high cloud types lead to the overestimated RSW and OLR anomalies. In the previous section it was shown that, over regions of strong ascent, HadAM4 produces excessive amounts of optically thick, high cloud leading to excessive SW and LW cloud radiative effects compared to observations. When such conditions arise anomalously in the equatorial Pacific during the 1987 El Niño, overestimated anomalies in both the RSW and OLR therefore result. In view of the results of the previous section, it is unsurprising to find that both the anvil and boundary layer mixing parametrizations influence the simulation of the interannual variations in cloud and the radiation budget. When the anvil parametrization is removed from HadAM4, the high cloud amount anomalies closely resemble those simulated by HadAM3, with only a very small increase in the magnitude of the anomalies in high, intermediate optical thickness cloud. Consequently, the RSW and OLR anomalies are also very similar to those simulated in HadAM3. When the new boundary scheme

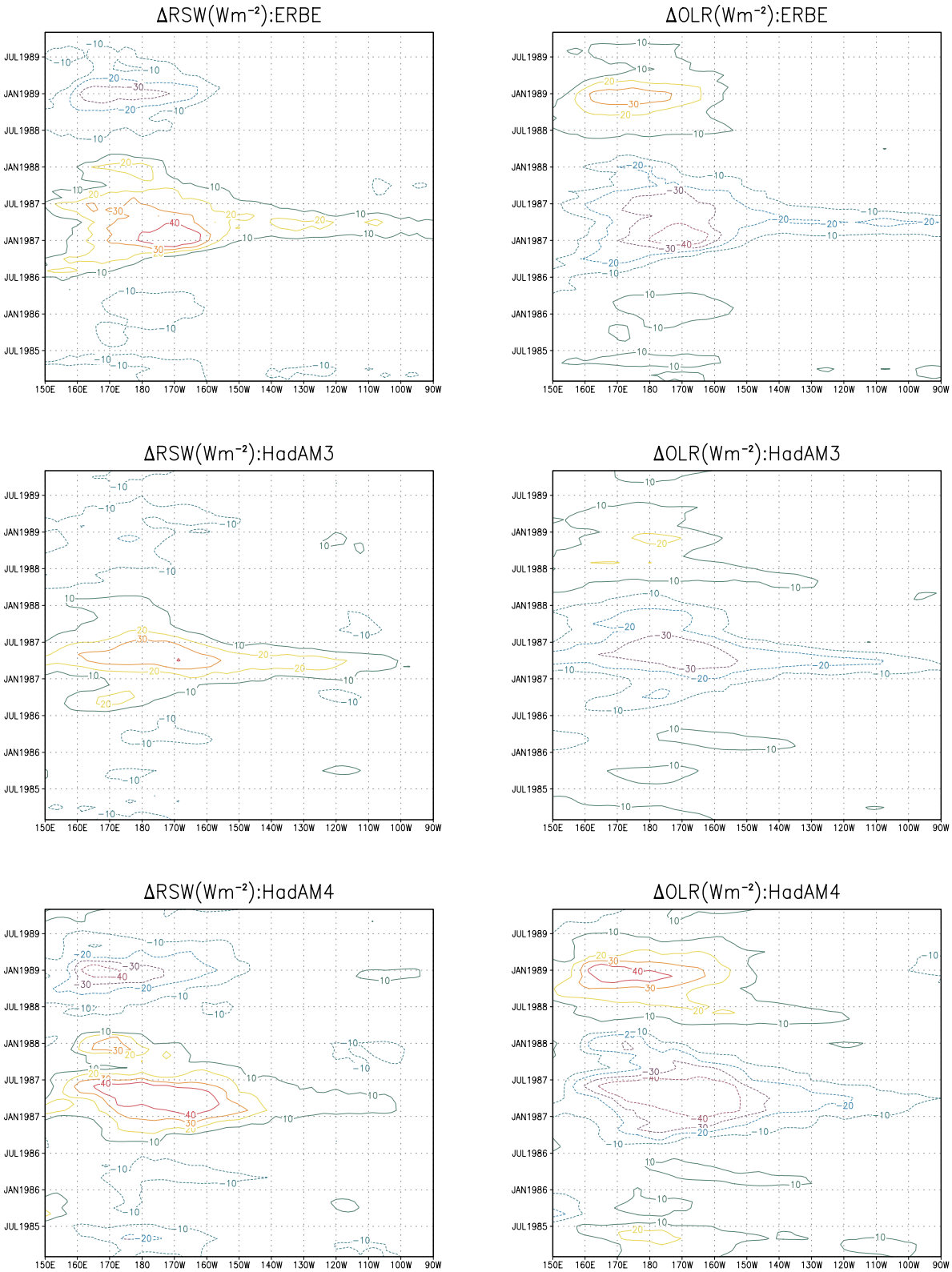


*Fig 10.* Hovmoller plots of the evolution of RSW and OLR anomalies over the equatorial Pacific for the period 1985–89 from (a), (b) observations, (c), (d) HadAM3 and (e), (f) HadAM4. Values are averaged over 5°N–5°S. The anomalies are calculated by removing the mean annual cycle and then applying a five-month running mean to emphasize the interannual variations.

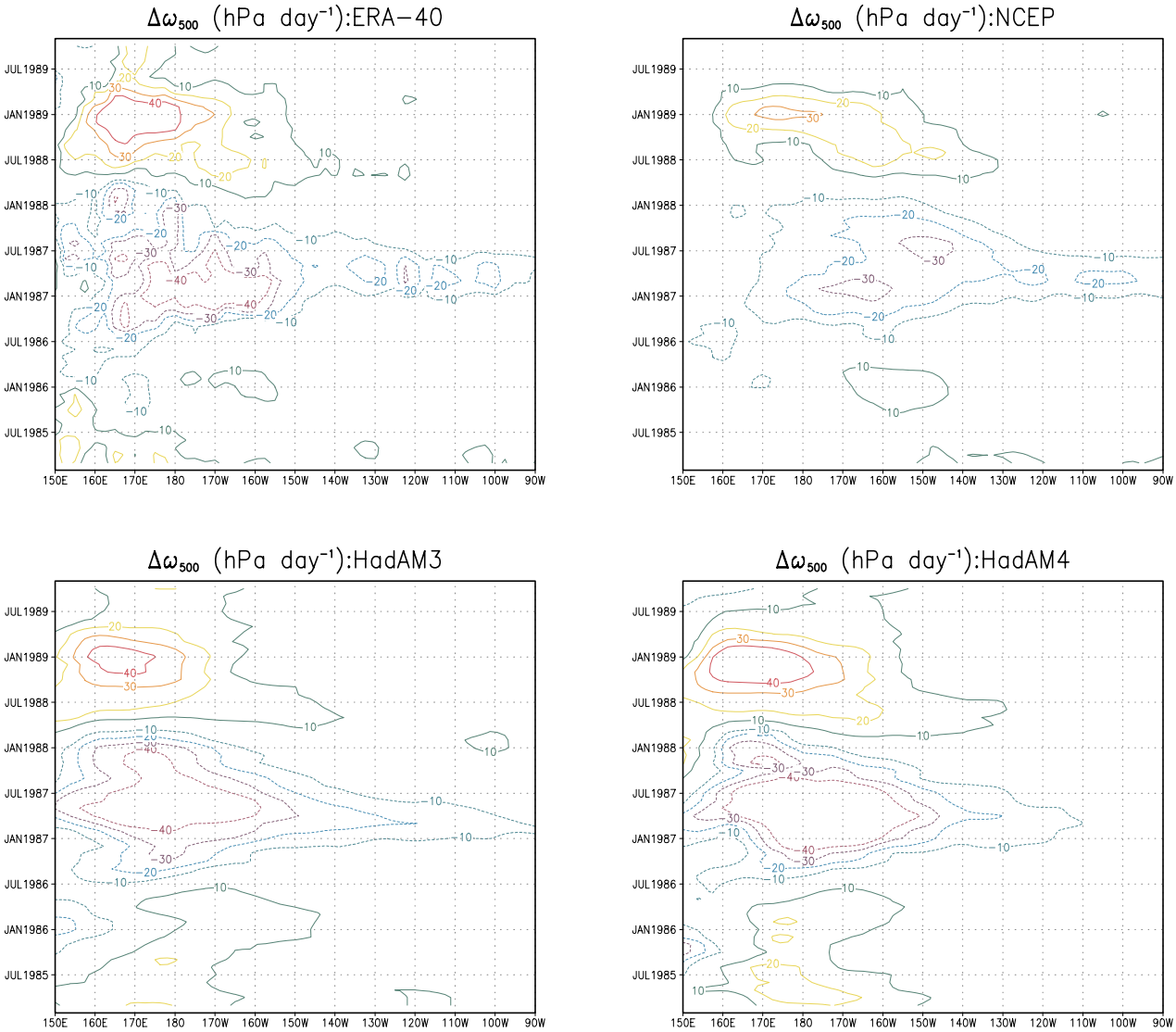


*Fig 11.* Hovmoller plots of the evolution of 500-hPa vertical velocity anomalies over the equatorial Pacific for 1985–89: (a) ERA-40 reanalyses, (b) NCEP reanalyses, (c) HadAM3 and (d) HadAM4.

is removed, the largest anomalies in both high cloud types (and, consequently, in the RSW and OLR) extend further eastward across the Pacific over the region of largest SST anomalies. This suggests that removing the boundary layer scheme results in a greater sensitivity to the SST anomalies, as the radiation budget anomalies over the area of the highest actual SSTs (which occur to the west of the dateline) are similar to those simulated in HadAM4.

It can thus be seen that the simulation of the ENSO-related interannual variability in clouds and radiation budget over the equatorial Pacific in the two models follows from the analysis in terms of dynamical regimes presented in previous sections. This result is analogous to that of Norris and Weaver (2001), who found that errors in the representation of interannual variability of low-level cloud over the mid-latitude North Pacific in the NCAR Community Climate Model followed directly from the model's inability to generate cloud in subsidence regimes.

## 6. Conclusions

An assessment of the simulation of tropical cloud in versions of the Hadley Centre climate model has been presented. In contrast to the more usual approach of comparing geographical distributions of observed and model climatologies, radiation budget parameters and cloud amounts are considered in terms of 'dynamical regimes' defined in terms of the SST and the large-scale vertical motion. The aim of this type of analysis is to consider clouds and cloud radiative effects in terms of physical processes. This provides a more thorough examination of the model's physical parametrizations and enables model deficiencies to be

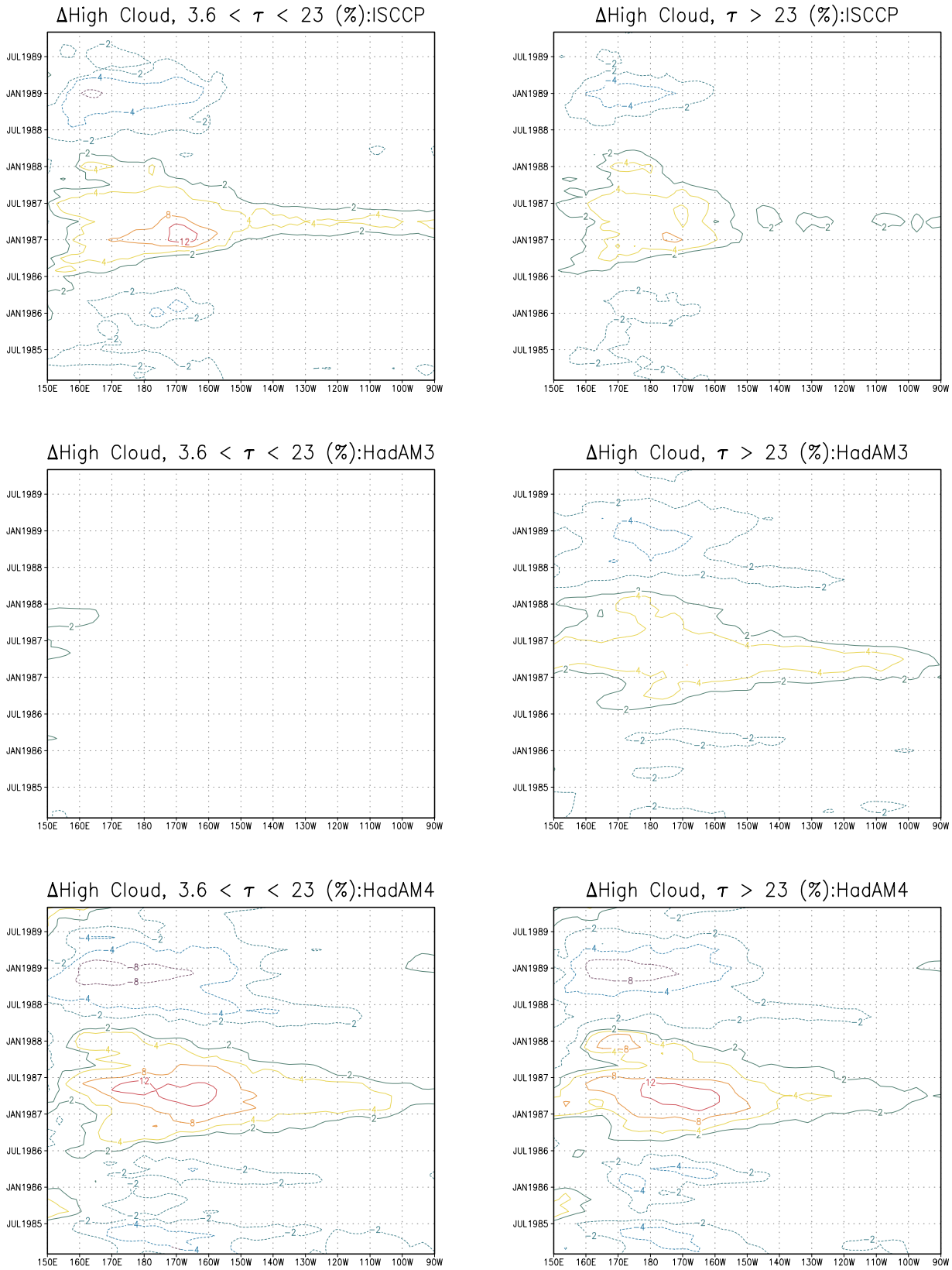


*Fig 12*. As Fig. 10 but for high cloud with $3.6 < \tau_{\mathrm{vis}} < 23$ and high cloud with $\tau_{\mathrm{vis}} > 23$.

identified more clearly. The analysis further benefits from the simulation in the model of cloud diagnostics that are directly comparable to quantities retrieved by ISCCP.

The analysis applied to HadAM3 reveals that over areas of warm SST and strong ascent this version of the model underestimates the amount of high, intermediate optical thickness cloud while at the same time overestimating the amount of the optically thickest high cloud. This results from the model's calculation of convective cloud amount and its failure to represent convective anvils. Over the coolest waters, in areas of large-scale subsidence the model significantly underestimates the amount of low-level cloud, a consequence of insufficient vertical resolution in the lower troposphere and the inadequacies of the boundary layer mixing scheme. In both these cases, overestimates of optically thick cloud (be it low- or high-level) compensate for these problems to some extent, leading to inconsistencies between the cloud and radiation budget simulations compared to observations.

The occurrence of such compensating errors is greatly reduced in a more recent version of the model (HadAM4), which includes a number of new, cloud-related parametrizations. This leads to a more consistent comparison with the satellite-derived radiation budget and cloud observations, although some deficiencies still remain. The most notable of these are the continued underestimate of low-level clouds in regions of large-scale descent and the overestimate of optically thick high cloud in areas of strong ascending motion, the latter of which leads to excessive SW and LW cloud radiative effects compared to ERBE data. The inability to generate low-level cloud arises despite the fact that the new boundary layer mixing scheme used in HadAM4, together with the increased vertical resolution, produces much more realistic boundary structures and it is likely that the utility of the scheme in this respect is limited by other aspects of the model's performance. In areas of strong ascent over warm waters, the new boundary layer scheme is shown to be responsible for rectifying the incorrect negative dependence of albedo and deep convective cloud on SST seen in HadAM3. A parametrization for the radiative effects of convective anvils results in the production of intermediate thickness high cloud previously absent in the model but also seems to increase deep convective cloud and to contribute to the excessive cloud radiative effects.

Examination of the simulation of interannual variations of clouds and the radiation budget associated with ENSO variability in the equatorial Pacific demonstrates that the ability of the two versions of the model to represent these changes follows directly from the previous analysis in terms of dynamical regimes. Thus, during the period of anomalously high SSTs in 1987, HadAM3 produces excessive amounts of the optically thickest high cloud which compensate for its lack of intermediate thickness cloud and result in fairly realistic top-of-atmosphere radiation budget anomalies. Similarly, HadAM4 overestimates both the intermediate thickness and optically thickest high cloud, leading to overestimated anomalies in the RSW and OLR.

It has been suggested that assessment in terms of dynamical regimes (Norris and Weaver, 2001) and of the ability to simulate current climate variability (Yao and Del Genio, 1999) should be more useful methods of climate model validation than simply comparing climatological mean states to observations, particularly if the aim is to assess a model's suitably for climate change studies. Such an approach allows the physical processes to be evaluated more reliably and should eventually provide greater understanding of the feedbacks operating within a model. This is particularly relevant to simulations of cloud, as cloud feedbacks are still not well understood. This paper has focused on simulations of the present-day climate. In a related study Williams et al. (2003), using a variation of the present methodology, have shown how the response of tropical cloud to increased greenhouse gases in the Hadley Centre model can be related to the model's simulation of interannual variability.

The techniques presented here have clearly proved useful for evaluating the simulation of tropical cloud in the Hadley Centre model and for assessing the impact of new physical parametrizations on these simulations. The method is relatively straightforward and could easily be applied to output from other climate models. It may thus prove useful for model intercomparison studies. This particular study has been restricted to present-day simulations of the tropical oceans. Clearly, it would be desirable to extend such methods to land areas and higher latitudes.

## 7. Acknowledgments

This work was supported by the Department of Environment, Food and Rural Affairs under contract PECD 7/12/37. We thank Keith Williams for performing some of the model simulations used in this study. The ERBE and ISCCP data were obtained from the National Aeronautics and Space Administration (NASA) Langley Research Center Atmospheric Sciences Data Center. The ERA-40 data were obtained from the ECMWF. The NCEP data were obtained from the National Oceanic and Atmospheric Administration–Cooperative Institute for Research in Environmental Sciences (NOAA–CIRES) Climate Diagnostics Center.

## References

Allan, R. P. and Ringer, M. A. 2003. Using reanalysis clear-sky OLR to improve the interpretation of cloud long-wave radiative effect. *Geophys. Res. Lett.* **30**(9), 1491 (doi:10.1029/2003GL017019).

Allan, R. P., Slingo, A. and Ringer, M. A. 2002. Influence of dynamics on the changes in tropical cloud radiative forcing during the 1998 El Niño. *J. Climate* **15**, 1979–1986.

Barkstrom, B. R. 1984. The Earth Radiation Budget Experiment (ERBE). *Bull. Am. Meteorol. Soc.* **65**, 1170–1185.

Bony, S., Sud, Y., Lau, K.-M. and Susskind, J. 1997a. Comparison and satellite assessment of NASA/DAO and NCEP-NCAR reanalyses over tropical ocean: atmospheric hydrology and radiation. *J. Climate* **10**, 1441–1462.

Bony, S., Lau, K.-M. and Sud, Y. C. 1997b. Sea surface temperature and large-scale circulation influences on tropical greenhouse effect and cloud radiative forcing. *J. Climate* **10**, 2055–2077.

Bony, S., Dufresne, J. L., Le Treut, H., Morcrette, J.-J. and Senior, C. A. 2003. On dynamic and thermodynamic components of cloud changes. *Clim. Dyn.* **22**, 71–86.

Bushell, A. C. and Martin, G. M. 1999. The impact of vertical resolution upon GCM simulations of marine stratocumulus. *Clim. Dyn.* **15**, 293–318.

Cess, R. D. and Potter, G. L. 1987. Exploratory studies of cloud radiative forcing with a general circulation model. *Tellus* **39**, 460–473.

Chou, M.-D. 1994. Coolness in the tropical Pacific during and El Niño episode. *J. Climate* **3**, 1129–1152.

Chou, C. and Neelin, J. D. 1999. Cirrus detrainment temperature feedback. *Geophys. Res. Lett.* **26**, 1295–1298.

Cusack, S., Edwards, J. M. and Kershaw, R. 1999. Estimating subgrid variance of saturation and its parametrization for use in a GCM cloud scheme. *Q. J. R. Meteorol. Soc.* **125**, 3057–3076.

Fu, R., Del Genio, A. D. and Rossow, W. B. 1994. Influence of ocean surface conditions on atmospheric vertical thermodynamic structure and deep convection. *J. Climate* **7**, 1092–1108.

Gibson, J. K., Kållberg, P., Uppala, S., Hernandez, A., Nomura, A. et al. 1997. ERA description. *ECMWF Re-analysis Project Report Series 1* (available from ECMWF).

Gregory, J. 1999. Representation of the radiative effect of convective anvils. *Hadley Centre Tech. Note 7* (available from the Met Office).

Harrison, E. P., Minnis, P., Barkstrom B. R., Ramanathan, V., Cess, R. D. et al. 1990. Seasonal variation of cloud radiative forcing derived from the Earth Radiation Budget Experiment. *J. Geophys. Res.* **95**, 18 687–18 703.

Hartmann, D. L. and Michelsen, M. L. 1993. Large-scale effects on the regulation of tropical sea surface temperatures. *J. Climate* **6**, 2049–2062.

Hartmann, D. L., Moy, L. A. and Fu, Q. 2001. Tropical convection and the energy balance at the top of the atmosphere. *J. Climate* **14**, 4495–4511.

Kalnay, E., Kanamitsu, M., Kistler, R., Collins, W., Deaven, D., et al. 1996. The NCEP/NCAR 40-year reanalysis project. *Bull. Am. Meteorol. Soc.* **77**, 437–471.

Kousky, V. E. 1989. The global climate for September–November 1988: High Southern Oscillation Index and cold episode characteristics continued. *J. Climate* **2**, 173–192.

Kousky, V. E. and Leetmaa, A. 1989. The 1986–87 Pacific warming episode: Evolution of oceanic and atmospheric anomaly fields. *J. Climate* **2**, 254–267.

Kristjánsson, J. E., Edwards, J. M. and Mitchell, D. L. 1999. A new parametrization for the optical properties of ice crystals for use in general circulation models of the atmosphere. *Phys. Chem. Earth* **107**, 231–236.

Lau, K.-M., Wu, H.-T. and Bony, S. 1997. The role of large-scale atmospheric circulation in the relationship between tropical convection and sea surface temperature. *J. Climate* **10**, 381–392.

Lock, A. 1998. The parametrization of entrainment in cloudy boundary layers. *Q. J. R. Meteorol. Soc.* **124**, 2729–2753.

Lock, A. P., Brown, A. R., Bush, M. R., Martin, G. M. and Smith, R. N. B. 2000. A new boundary layer mixing scheme. Part I: Scheme description and single column model tests. *Mon. Wea. Rev.* **128**, 3200–3217.

Martin, G. M., Bush, M. R., Brown, A. R., Lock, A. P. and Smith, R. N. B. 2000. A new boundary layer mixing scheme. Part II: Tests in climate and mesoscale models. *Mon. Wea. Rev.* **128**, 3200–3217.

Norris, J. R. and Weaver, C. P. 2001. Improved techniques for evaluating GCM cloudiness applied to the NCAR CCM3. *J. Climate* **14**, 2540–2550.

Oort, A. H. and Yienger, J. J. 1996. Observed interannual variability in the Hadley circulation and its connection to ENSO. *J. Climate* **9**, 2751–2767.

Pope, V. D., Gallani, M., Rowntree, P. R. and Stratton, R. A. 2000. The impact of new physical parametrizations in the Hadley Centre climate model—HadAM3. *Clim. Dyn.* **16**, 123–146.

Rossow, W. B. and Schiffer, R. A. 1991. ISCCP cloud data products. *Bull. Am. Meteorol. Soc.* **72**, 2–20.

Rossow, W. B. and Schiffer, R. A. 1999. Advances in understanding clouds form ISCCP. *Bull. Am. Meteorol. Soc.* **80**, 2261–2287.

Simmons, A. and Gibson, R. 1999. *The ERA-40 project plan* (available from ECMWF).

Sun, D.-Z. and Trenberth, K. E. 1998. Coordinated heat removal from the equatorial Pacific during the 1986–87 El Nino. *Geophys. Res. Lett.* **25**, 2659–2662.

Trenberth, K. E. and Guillemot, C. J. 1998. Evaluation of the atmospheric moisture and hydrological cycle in the NCEP/NCAR reanalysis. *Clim. Dyn.* **14**, 213–231.

Tselioudis, G. and Jakob, C. 2002. Evaluation of mid-latitude cloud properties in a weather and a climate model: Dependence on dynamic regime and spatial resolution. *J. Geophys. Res.* **107**, 4781 (doi:10.1029/2002JD002259).

Webb, M. J., Senior, C. A., Bony, S. and Morcrette, J.-J. 2001. Combining ERBE and ISCCP data to assess clouds in the Hadley Centre, ECMWF and LMD atmospheric models. *Clim. Dyn.* **17**, 905–922.

Williams, K. D., Ringer, M. A. and Senior, C. A. 2003. Evaluating the cloud response to climate change and current climate variability. *Clim. Dyn.* **20**, 705–721.

Wilson, D. R. and Ballard, S. P. 1999. A microphysically based precipitation scheme for the UK Meteorological Office Unified Model. *Q. J. R. Meteorol. Soc.* **125**, 1607–1636.

Yao, M.-S. and Del Genio, A. D. 1999. Effects of cloud parametrization on the simulation of climate changes in the GISS GCM. *J. Climate* **12**, 761–779.

Zender, C. S. and Kiehl, J. T. 1997. Sensitivity of climate simulations to radiative effects of tropical anvil structure. *J. Geophys. Res.* **102**, 23 793–23 803.

Zhang, C. 1993. Large-scale variability of atmospheric deep convection in relation to sea surface temperature in the tropics. *J. Climate* **6**, 1898–1913.